Nearest-Neighbor Distribution Functions for Impenetrable Particles in One to Three Dimensions

James Ross Macdonald

Department of Physics and Astronomy, University of North Carolina, Chapel Hill, North Carolina 27599-3255
(Received: October 31, 1991)

In several interesting recent papers, S. Torquato and his associates presented specific expressions for the D-dimensional hard-sphere nearest-neighbor probability density distribution function, P_{NN}, and the mean nearest-neighbor particle separation, R_{NN}, for $D = 1$, 2, and 3. These expressions, which have been known since 1981, are closely related to general expressions of scaled particle theory given by Reiss and co-workers in 1959 and 1974. Here, the consequences of four different choices for the basic probability function, G, needed in calculating P_{NN} and R_{NN}, are explored with particular emphasis on the $D = 3$ situation. In addition to the particular G used by Torquato, which was associated with the Carnahan-Starling equation of state, and the different one used by the author in 1981, two other choices are proposed. One of these is an improved version of that used by Torquato, and the other is greatly simplified. It is shown that, as far as the dependences of P_{NN} on distance from a particle boundary and those of P_{NN} and R_{NN} on particle density are concerned, even the simplified choice is quite adequate to yield results which cannot be practically distinguished from those following from the improved choice for G or that used by Torquato.

I. Introduction and Background

Much analysis of the behavior of an assembly of hard spheres in thermodynamic equilibrium has been carried out because, for example, such a system is a useful approximation to the behavior of rare gases and monatomic liquid metals. The results of such analysis, which is often concentrated on deriving an appropriate equation of state, are also pertinent to many other problems in the physical and biological sciences, ranging from stellar dynamics to amorphous solids. An important quantity in such work is the nearest-neighbor probability density function. Here, attention is devoted to this quantity rather than directly to equation of state results.

In a series of recent papers,[1-3] S. Torquato and his associates (abbreviated TLR) claimed to present for the first time specific expressions for the hard-particle nearest-neighbor distribution function, $P_{NN}(\phi,x)$, and mean nearest-neighbor particle separation, $R_{NN}(\phi)$, in one to three dimensions. Unfortunately, these authors were unaware of relevant earlier work on the subject. Here, I both compare the TLR predictions for these quantities (when corrected for errors) with those of earlier workers and, in addition, propose a useful simplification of the results. Part of the problem, and interest in these quantities, arises because although they can be calculated exactly for one dimension ($D = 1$), it seems unlikely that this is possible for hard disks ($D = 2$) and hard spheres ($D = 3$). Thus, different physical assumptions or approximations can lead to different results for $D = 2$ and 3. The present work is closely related to a more detailed study which has been submitted for publication.[4]

Let the "diameter" of a hard particle (referred to as a sphere for all D values for simplicity) be denoted by σ. Then the normalized distance variable, $x \equiv r/\sigma$, involves the distance r from the center of a hard sphere to an arbitrary point in an assembly of equisized hard spheres, taken homogeneous in the large and in thermodynamic equilibrium. Thus, the minimum physically allowable value of the presently defined x is 1, and we need to be concerned only with quantities defined from $x = 1+$ to ∞. Therefore, the distinct functions G_V and G_P introduced by TLR are identical in this range, and their distinction is of no consequence in calculating P_{NN} and R_{NN} (for $x \geq 1+$). The packing fraction, the reduced density ϕ, is defined as ρV_D, where V_D is the volume of a particle of diameter σ and $\rho \equiv N/V$, the number density. The maximum allowed value of ρ is $\sqrt{2}\sigma^{-3}$ for $D = 3$, the hexagonal close-packed value. The corresponding maximum value of ϕ, ϕ_c, is $\sqrt{2}\pi/6 \simeq 0.740\,48$. In general

$$\phi = \pi^{D/2}\rho(\sigma/2)^D/\Gamma\{1 + (D/2)\} \quad (1)$$

where Γ is the gamma function.

Now define $J(n,\phi)$, the nth moment of P_{NN}

$$J(n,\phi) \equiv \int_1^\infty y^n P_{NN}(\phi,y)\, dy \quad (2)$$

When $n = 0$, we must have $J(0,\phi) = 1$, the normalization condition for the dimensionless probability density P_{NN}. But when $n = 1$, $J(1,\phi) \equiv R_{NN}(\phi) \equiv \langle r \rangle/\sigma$, the normalized mean nearest-neighbor distance, the first moment of the distribution. It is thus clear that once an expression for P_{NN} is given, the corresponding R_{NN} follows immediately.

A general expression closely related to the present $P_{NN}(\phi,x)$ formula defined below appears in the original scaled particle theory work of 1959[5] and was further discussed and generalized by Reiss and Casberg[6] in 1974. Although no explicit results for $D = 2$ and 3 were presented in these works, a general expression for P_{NN}, equivalent to the generalized result of Reiss and Casberg (with their λ set to σ), was independently derived by the author in 1981[7] and was specialized for $D = 1$-3 for both P_{NN} and R_{NN}.

A function which plays the crucial role in determining P_{NN} has usually been denoted by G in the literature of the present subject. In its unnormalized form this function, $G(\phi,x)$, was termed the central function of scaled particle theory by Reiss and Casberg,[6] and it was denoted by TLR as the conditional pair distribution function and defined[2] as "the radial distribution function for a special binary mixture of spheres, namely, one for a single test particle of radius $r - \sigma/2$ and an actual inclusion of diameter σ at contact, i.e., when such particles are separated by the distance r". In the 1981 work[7], $G(\phi,x)$ was approximated by the inverse relative free volume, $\Lambda_f(\phi) \equiv v_f^{-1}$. The free volume, v_f, is that available for particle motion and was taken zero at the density of crystalline close packing,[8,9] $\phi \equiv \phi_c$. The 1981 work and results

(1) Torquato, S.; Lu, B.; Rubinstein, J. *J. Phys. A: Math. Gen.* **1990**, *23*, L103.

(2) Torquato, S.; Lu, B.; Rubinstein, J. *Phys. Rev. A* **1990**, *41*, 2059. There appear to be extraneous h and $(1 - \eta)$ terms in eqs 4.33 and 4.34 which do not follow from the use of eqs 2.18 and 2.20 from which they were derived. Luckily, they make no difference in the result obtained for P_{NN} in the 3D case. There is a missing factor of η^2 in eq 5.6 and a missing set of brackets in eq 5.13. In the statement on p 2074, "At fixed ϕ_2, l/σ increases with increasing D, as expected," the word "increases" should be changed to "decreases".

(3) Torquato, S.; Lee, S. B. *Physica A* **1990**, *167*, 361. There is a missing minus sign in the exponential argument of eq 46.

(4) Macdonald, J. R. Submitted to *Phys. Rev. A*.

(5) Reiss, H.; Frisch, H. L.; Lebowitz, J. L. *J. Chem. Phys.* **1959**, *31*, 369.

(6) Reiss, H.; Casberg, R. V. *J. Chem. Phys.* **1974**, *61*, 1107.

(7) Macdonald, J. R. *Mol. Phys.* **1981**, *44*, 1043.

0022-3654/92/2096-3861$03.00/0

will be referred to by the abbreviation JRM.

The general expression for P_{NN} can be written concisely and explicitly in terms of the functions

$$F(\phi,x) \equiv D\cdot 2^D \phi x^{D-1} G(\phi,x) \tag{3}$$

and

$$I(\phi,x) = \int_1^x F(\phi,y)\, dy \tag{4}$$

Then

$$P_{NN}(\phi,x) = F(\phi,x)\exp[-I(\phi,x)]U_0(x-1) \tag{5}$$

where U_0 is the unit step function. Thus, it follows that an expression for P_{NN} may be found given any plausible expression for the basic function $G(\phi,x)$. But it is worth reiterating that for $D > 1$ no exact expressions for $G(\phi,x)$ are known. From the form of the eq 5 result, P_{NN} is clearly normalized. The preexponential function $F(\phi,x)$ has a simple physical interpretation, although this is insufficient (so far!) to allow it to be calculated exactly for $D > 1$. The conditional probability of finding a particle within the spherical shell of normalized thickness dx and inner normalized radius x (≥ 1) is[2,4] just $F(\phi,x)\,dx$.

There are three further general equations of importance in the present context. Define $g_r(\phi,x)$ as the ordinary radial distribution function; its value at contact is thus $g_r(\phi,1)$. Then for hard particles in equilibrium the equation of state is given in terms of $g_r(\phi,1)$ by[5,6,10-12]

$$Z(\phi) \equiv P/\rho kT = 1 + 2^{D-1}\phi g_r(\phi,1) \tag{6}$$

where P is the pressure of the system and k and T have their usual meanings. In addition,[5,11,12] we have

$$G(\phi,\infty) = Z(\phi) \tag{7}$$

and

$$G(\phi,1) = g_r(\phi,1) \tag{8}$$

Thus, $G(\phi,x)$ only equals the radial distribution function at particle contact, $x = 1$. For the $D = 1$ situation, matters are particularly simple. Then the relations $G(\phi,x) = g_r(\phi,x) \equiv g_r(\phi) = \Lambda_f(\phi) = (1-\phi)^{-1}$ are exact. The choice $G(\phi,x) = \Lambda_f(\phi)$ for $D = 2$ and 3 in the 1981 work[7] was based on extrapolation of these relations to higher dimensions.

For $D = 1$, where an exact solution is possible, TLR found the same results as did the author in 1981.[7] For $D = 2$, the results found for P_{NN} and R_{NN} were very similar over a wide range of ϕ. (In order to achieve such close agreement, however, the TLR expressions had to be corrected for a sign error in their eqs 5.13, 5.14, and 6.9.[4]) These comparisons and corrections are discussed in more detail in ref 4. There are somewhat greater differences between the TLR and 1981 JRM predictions for $D = 3$ than for $D = 2$, reflecting progressive loss in accuracy of the $G(\phi,x) = \Lambda_f(\phi)$ approximation used in ref 7 as D increases beyond 1. Therefore, only $D = 3$ comparisons are considered herein, and the interested reader is referred to ref 4 for more details for all three choices of D.

Four possible choices for the basic $G(\phi,x)$ function are defined and discussed in the next section. Then in section III the P_{NN} and R_{NN} responses following from these choices are compared, and new conclusions are reached concerning the accuracy and utility of the various choices.

II. Four Choices for $G(\phi,x)$ When $D = 3$

In addition to comparing the JRM and TLR choices for $G(\phi,x)$ in terms of their resulting $P_{NN}(\phi,x)$ and $R_{NN}(\phi)$ responses, I shall compare two new choices as well. The main $G(\phi,x)$ expression presented by TLR, $G_{PT}(\phi,x)$, is based on the Carnahan–Starling equation of state (abbreviated CS EOS) for hard spheres, considered by these authors to be the approach which led to their best results. Let us write G in the following general form[5]

$$G_m(\phi,x) = a_m(\phi) + x^{-1}b_m(\phi) + x^{-2}c_m(\phi) \tag{9}$$

Then the $m = 1$–4 choices are defined by

$$G_{PT}(\phi,x) \equiv G_1(\phi,x) \tag{10}$$

with

$$a_1(\phi) \equiv (1+\phi)/(1-\phi)^3; \quad b_1(\phi) \equiv -\phi(3+\phi)/\{2(1-\phi)^3\}; \quad c_1(\phi) \equiv \phi^2/\{2(1-\phi)^3\}$$

$$G_{PTC}(\phi,x) \equiv G_2(\phi,x) \tag{11}$$

with

$$a_2(\phi) \equiv (1+\phi+\phi^2-\phi^3)/(1-\phi)^3; \quad b_2(\phi) \equiv -3\phi(1+\phi)/\{2(1-\phi)^3\}; \quad c_2(\phi) \equiv \phi^2(1+2\phi)/\{2(1-\phi)^3\}$$

$$G_3(\phi,x) = g_r(\phi,1) = (1-\phi/2)/(1-\phi)^3 \tag{12}$$

$$G_4(\phi,x) = \Lambda_f(\phi) = 1/[1-(29/14)\phi + 0.9736\phi^2] \tag{13}$$

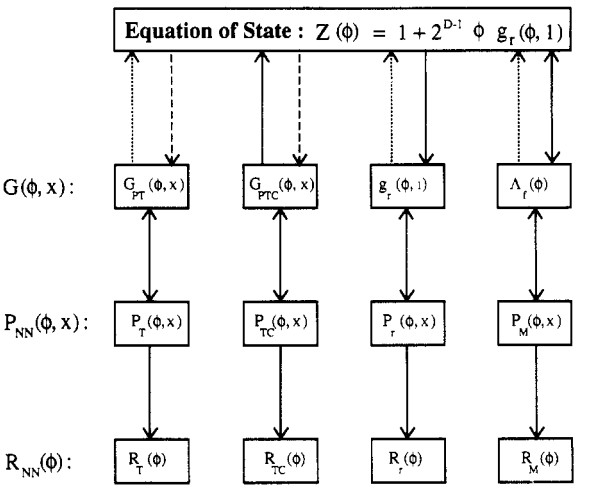

Figure 1. Block diagram flow chart showing relations between four different choices of the basic function $G(\phi,x)$ and other related quantities. Here G_{PT} is the original TLR choice; G_{PTC} is an improved version of G_{PT}; $g_r(\phi,1)$ is the contact value of the radial distribution function; and Λ_f is an expression for the relative inverse free volume used in the 1981 JRM work. See text for discussion of the meanings of the various types of connecting lines. Here ϕ is a normalized particle density, the packing fraction, and x is the normalized distance measured from a particle center.

The four choices and their corresponding P_{NN} and R_{NN} results, using abbreviated symbols, are summarized in the block diagram of Figure 1. In this diagram, arrows show the direction of a possible transformation, solid lines indicate exact and/or consistent transformations, dotted lines denote inconsistent transformations, and dashed ones represent transformations that involve the solution of an inverse problem and thus such transformations are correspondingly uncertain and nonunique.

The first choice above and that at the left of the diagram defines the TLR solution. Since the derivation of $G(\phi,x)$ from an expression for $Z(\phi)$ involves the solution of an ill-defined (ill-posed) inverse problem, the G_{PT} result used by TLR for the CS EOS is correspondingly uncertain. In addition, although their expression for G_{PT} satisfies eq 8, since $G_{PT}(\phi,1) = (a_1 + b_1 + c_1) = g_r(\phi,1)$ as given in eq 12 for the CS EOS, it does not satisfy eq 7 even though an equation equivalent to eq 7 was given by these authors. Further, although the expression for $G(\phi,x)$ listed by TLR for scaled particle theory[5,11] does satisfy both eqs 7 and 8, that which they give for the Percus–Yevick solution does not.

Since the TLR G_{PT} is inconsistent, it is worthwhile modifying it to make it consistent with both eqs 7 and 8. Such modification

(8) Andrews, F. C. *J. Chem. Phys.* **1975**, *62*, 272.
(9) Andrews, F. C. *J. Chem. Phys.* **1976**, *64*, 1941.
(10) Hansen, J. P.; McDonald, I. R. *Theory of Simple Liquids*, 2nd ed.; Academic Press: New York, 1986.
(11) Helfand, E.; Frisch, H. L.; Lebowitz, J. L. *J. Chem. Phys.* **1961**, *34*, 1037.
(12) Reiss, H.; Schaaf, P. *J. Chem. Phys.* **1989**, *91*, 2514.

yields choice 2, G_{PTC}, a corrected expression for $G(\phi,x)$ for the CS EOS. Although there is still an element of arbitrariness in the result given in eq 11, it is worth noting that $b_2(\phi)$ is identical to the corresponding term in the expression for $G(\phi,x)$ for scaled particle theory.[5] It is thus plausible to expect G_{PTC} to be superior to G_{PT}, even though the details of the G_{PTC} ϕ and the x dependences are almost certainly not exact.

The third choice ignores x dependence in $G(\phi,x)$ and uses just the contact value of the radial distribution function, thus guaranteeing satisfaction of eq 8. This approach has the additional virtue that such a choice is always possible whenever an EOS expression is available, and thus no inverse problem estimate needs to be used. But, of course, it has the disadvantage that, like choice 1, eq 7 is not satisfied. How much accuracy is lost by making a choice of this kind where the x dependence of $G(\phi,x)$ is ignored? The answer is "very little" as far as P_{NN} and R_{NN} are concerned. The reason is that the present choice leads to the same contact value of P_{NN}, $P_{NN}(\phi,1)$, as do the first two choices because they all satisfy eq 8, and in addition, because all P_{NN} curves are normalized to unity there turns out to be little room for differences between the various predictions. This conclusion is quantified in the next section.

Finally, choice 4 involves the inverse relative free volume function, $\Lambda_f(\phi)$, one where neither eq 7 nor eq 8 is satisfied. The coefficient of the ϕ term in eq 13 is determined from the exact third virial expansion term, and the remaining coefficient value ensures that $\Lambda_f(\phi)$ has a pole at $\phi = \phi_c$. Thus, the present expression for $\Lambda_f(\phi)$ is not at all directly associated with the CS EOS. It involves, however, an EOS which turns out to approximate very well the CS EOS.[8] Further, because there is no x dependence, the transformation from $\Lambda_f(\phi)$ to the corresponding EOS, and the reverse transformation, are exact. Because eqs 7 and 8 are not satisfied, however, a dotted line is shown for the transformations where $G(\phi,x)$ is set to $\Lambda_f(\phi)$. Further, because this approach leads to a value of $P_{NN}(\phi,1)$ possibly considerably different from that of choices 1 and 2, we expect larger differences between the $P_{NN}(\phi,x)$ curves of choices 1 and 2 and the 1981 $\Lambda_f(\phi)$ predictions.

III. Comparison of Results for P_{NN} and R_{NN}

Although some graphical comparisons of TLR and JRM D = 2 and 3 results are presented in ref 4, here only holistic numerical comparisons will be made. To do so, we shall use a χ^2 comparison method.[13] First, for two sets of numbers, A_i and B_i, with i = 1, 2, ..., N, define

$$\chi^2(A,B) \equiv \sum_{i=1}^{N} [A_i - B_i]^2/B_i \qquad (14)$$

This expression may be used to yield a chi-square probability measure of the equality of the two data sets when the B_i represent values drawn from a known distribution and the A_i are drawn from an unknown distribution which may or may not be the same as that of the B_i. Here, however, we shall compare, for example, a set of $P_{NN}(\phi,x_i)$, say the $P_{TC}(\phi,x_i)$ of Figure 1, with corresponding TLR $P_T(\phi,x_i)$ values. Since such a comparison is deterministic, however, and involves systematic, not random, differences, no probability measure is appropriate. On the other hand, if $A_i = [P_{NN}(\phi,x_i)]_{MC}$ represented Monte Carlo measurements and $B_i = [P_{NN}(\phi,x_i)]_{TH}$ represented theoretical results, such a measure would be applicable.

Here, we shall use χ^2 values just as measures of the differences between two approximate representations of the same quantity. In order to remove most of the dependence of χ^2 on N, it is useful to define

$$\chi_N^2(A,B) \equiv \chi^2(A,B)/M_N \qquad (15)$$

where M_N is a normalization factor. We shall use $M_N = N - 1$ for $N > 1$ and $M_N = 1$ for $N = 1$. A weighting alternative is to replace the B_i in the denominator of eq 15 by $[B_i]^{2\xi}$ and set $M_N = \sum_{i=1}^{N} [B_i]^{-2\xi}$ with $0 < \xi < 2$. Results with $\xi = 0.5$ are similar to those with $M_N = N - 1$, while the $\xi = 1$ choice leads to smaller values of χ_N^2.

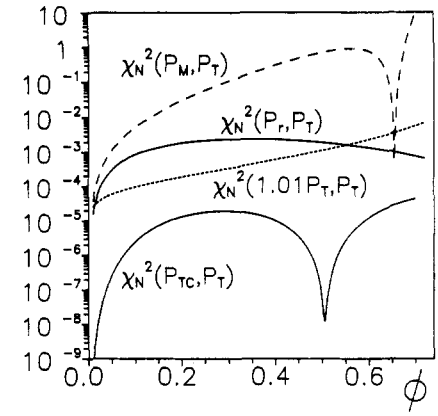

Figure 2. Overall comparisons for D = 3 between various pairs of response functions (see Figure 1 for identifications). Calculations of χ_N^2 were carried out, at constant ϕ, over a wide range of x values. Here $\chi_N^2(A,B)$ is a normalized chi-square function and ϕ is a normalized particle density, the packing fraction.

Figure 2 shows results for various pair comparisons for the four different P_{NN} nearest-neighbor distributions associated with the four $G(\phi,x)$ choices. These results were calculated using 800 x values, uniformly distributed between x = 1 and that particular x which led to a value of P_{NN} 1000 times smaller than its initial value. Results were found to be very nearly independent of N for $N \gg 1$. First, we see that the overall differences between P_{TC} and P_T are completely negligible, in spite of their different ϕ dependences. Thus, it does not matter whether the other comparisons are made using P_T or P_{TC} as a reference. Incidentally, for $\phi > 0.494$, where 0.494 is the freezing point of a hard-sphere assembly, the system contains regions of both long- and short-range order. Then under some circumstances, Monte Carlo results show that it can follow a path as ϕ increases which ends at $\phi \simeq 0.64$, termed random close packing, a condition where the pressure has a pole and there is no free volume available. Although this possibility is discussed in detail in ref 4, since it was not considered in either the TLR or the original JRM work, it is ignored here and the curves of Figure 2 are extended to ϕ = 0.7.

Second, to provide a point of reference, the dotted line in the figure shows the comparison between $1.01P_T$ and P_T. Next, the P_r and P_T comparison indicates that, for practical purposes, no significant accuracy is lost when the x dependence of $G(\phi,x)$ is completely ignored, provided that the contact value of the P_{NN} expression used is equal to that obtained when the x dependence is not ignored (e.g., provided that eq 8 holds). Incidentally, when $P_r(\phi,x)$ and $P_T(\phi,x)$ are plotted together on the same graph versus x, their lines cannot be distinguished from each other. On the other hand, the P_M and P_T comparison indicates appreciable differences between the two distributions except at very small ϕ and near $\phi \simeq 0.66$.

Finally, one may use the same apparatus to compare different $R_{NN}(\phi_i)$ results. Although $R_r(\phi)$ and $R_M(\phi)$ expressions may be obtained in closed form[4,7] because the P_{NN} distributions used in eq 2 with n = 1 do not involve the integration variable y, numerical quadrature is needed to obtain R_{TC} and R_T values. Further, since for the R_{TC} and R_T comparison one deals with very small differences, it is important to carry out the integration to very high accuracy. It was found that increasing the number of generalized trapezoidal integration points above 20000 geometrically distributed values made no difference in the comparisons. The integration range extended from y = 1 to a value of y for which $yP_{NN}(\phi,y)$ was negligibly small. With N = 691 values covering the range $0.01 \le \phi_i \le 0.7$, the following results were obtained: $\chi_N^2(R_{TC},R_T) \simeq 9.75 \times 10^{-9}$, $\chi_N^2(R_r,R_T) \simeq 3.25 \times 10^{-6}$, $\chi_N^2(R_M,R_T) \simeq 4.90 \times 10^{-5}$, and $\chi_N^2(R_M,R_r) \simeq 3.00 \times 10^{-5}$. Thus, for the mean nearest-neighbor comparison there is absolutely no significant difference between the $R_r(\phi)$, $R_{TC}(\phi)$, and $R_T(\phi)$ results. Further, because of the effect of integration, the somewhat

(13) Press, W. H.; Flannery, B. P.; Teukolsky, S. A.; Vetterling, W. T. *Numerical Recipes*; Cambridge University Press: New York, 1986; p 470.

significant differences between $P_M(\phi,x)$ and $P_T(\phi,x)$ lead to R_M and R_T results which are not significantly different for any practical purpose.

The present results indicate that although G_{PT} and G_T depend on ϕ differently and G_{PT} should be superior to G_T, their differences actually lead to P_{NN} and R_{NN} results which are far too close together to allow any discrimination. As far as R_{NN} is concerned, it makes no significant difference which of the four $G(\phi,x)$ choices is used. Although the best choice for P_{NN} for the CS EOS seems to be P_{TC}, the use instead of P_r induces only negligible differences and has the virtue that the required $g_r(\phi,1)$ function is immediately available from this or any other EOS of interest.

Conformational Equilibrium in the Alanine Dipeptide in the Gas Phase and Aqueous Solution: A Comparison of Theoretical Results

Douglas J. Tobias† and Charles L. Brooks III*

Department of Chemistry, Carnegie Mellon University, Pittsburgh, Pennsylvania 15213
(Received: November 4, 1991)

The acetyl and methyl amide blocked alanine amino acid, commonly referred to as the alanine dipeptide, has often been used as a model in theoretical studies of backbone conformational equilibria in proteins. In order to evaluate the solvent effects on the conformational equilibrium of the dipeptide, we have used molecular dynamics simulations with holonomic backbone dihedral angle constraints and thermodynamic perturbation theory to calculate free energy profiles along paths connecting four important conformations of the dipeptide in the gas phase and in water. We found that the extended β conformation is the most stable both in the gas phase and in water. The C_{7ax} conformation (seven-membered ring closed by a hydrogen bond with axial methyl group) is less stable than the β conformation by 2.4 kcal/mol in the gas phase and 3.6 kcal/mol in water. The right- and left-handed α helical conformations, α_R and α_L, are less stable than the β conformation by 9.1 and 11.6 kcal/mol, respectively, in the gas phase. However, in aqueous solution the α_R and α_L conformations are less stable than the β conformation by only 0.2 and 4.1 kcal/mol, respectively. Thus, we found, as others have previously, that there is a marked solvent effect on the backbone conformational equilibrium. We have determined the energetic and entropic contributions to the free energies to explain the relative stabilities of the dipeptide conformations in terms of differences in peptide–peptide and peptide–solvent interactions. Finally, we have compared our results to the results of several previous theoretical studies of the alanine dipeptide.

Introduction

The alanine dipeptide[1] (see Figure 1) has served as a paradigm for theoretical studies of backbone conformational equilibria in proteins. This is because the dipeptide contains many of the structural features of the protein backbone (the flexible ϕ and ψ dihedral angles, two amide peptide bonds whose NH and CO groups are capable of participating in hydrogen bonds with each other and with polar solvent molecules, and a methyl group attached to the α carbon that is considered representative of the side chains in all non-glycine or proline amino acids), yet it is small enough to be studied thoroughly in the gas phase using high-level quantum chemical calculations[2] and in aqueous solution using classical computer simulations (Monte Carlo (MC) and molecular dynamics (MD)) or statistical mechanical integral equation theories.[3-8]

There have been several previous studies of the thermodynamics of conformational equilibria in the alanine dipeptide in water. Mezei et al.[4] used MC simulations to calculate the relative solvation thermodynamics of the C_{7ax}, α_R, and P_{II} ($\phi \approx -80°$, $\psi \approx 150°$) conformations. The full ϕ,ψ free energy surface for the dipeptide in water was determined in the studies by Pettitt and Karplus[6,7] and by Anderson and Hermans.[8] Pettitt and Karplus used a statistical mechanical integral equation theory, the extended RISM theory with a superposition approximation, to compute the free energy surface. Pettitt and Karplus also used finite difference temperature derivatives of the free energy to determine the corresponding internal energy and entropy surfaces. Anderson and Hermans employed MD simulations with specialized sampling methods to construct the conformational probability distribution from which they derived the free energy surface.

All three studies agree qualitatively in the sense that they all show that there is a marked solvent effect on conformational equilibria in the alanine dipeptide. Generally speaking, the aqueous solvent appears to "flatten" the ϕ,ψ free energy surface, decreasing the free energy difference between conformations that differed by large energies on the vacuum surface and lowering the barriers separating those conformations. It is interesting that the results of Anderson and Hermans for the dipeptide ϕ,ψ probability distribution in water actually match the observed protein distribution quite well.[8] This comparison suggests that the effects of the solvent on the conformational distribution of the dipeptide are similar to the effects of long-range and specific side chain interactions on the backbone in proteins. This profound global solvent modification of the conformational free energy surface affects not only the relative stabilities of the various conformations, but also the dynamics and fluctuations within the minima and the kinetics of interconversion of different species. Thus, we expect the solvent to play an important role in determining the mechanism of the folding/unfolding of small peptides in solution. Unfortunately, the quantitative details of the results of the three studies cited above differ, indicating a subtle model

† Present address: Department of Chemistry, University of Pennsylvania, Philadelphia, PA 19104.

(1) The alanine dipeptide is the blocked alanine residue, Ac-ala-NHMe, where Ac is the N-terminal blocking group, $COCH_3$, and NHMe is the C-terminal blocking group, $NHCH_3$.

(2) Head-Gordon, T.; Head-Gordon, M.; Frisch, M. J.; Brooks, C. L. III; Pople, J. A. *J. Am. Chem. Soc.* **1991**, *113*, 5989 and references therein.
(3) Rossky, P. J.; Karplus, M. *J. Am. Chem. Soc.* **1979**, *101*, 1913.
(4) Mezei, M.; Mehrotra, P. K.; Beveridge, D. L. *J. Am. Chem. Soc.* **1985**, *107*, 2239.
(5) Brady, J. Karplus, M. *J. Am. Chem. Soc.* **1985**, *107*, 6103.
(6) Pettitt, B. M.; Karplus, M. *Chem. Phys. Lett.* **1985**, *121*, 194.
(7) Pettitt, B. M.; Karplus, M. *J. Phys. Chem.* **1988**, *92*, 3994.
(8) Anderson, A.; Hermans, J. *Proteins* **1988**, *3*, 262.
(9) Tobias, D. J.; Brooks, C. L. III *Biochemistry* **1991**, *30*, 6059.

0022-3654/92/2096-3864$03.00/0